Dyck's surfaces, systoles, and capacities

Mikhail G Katz, Stéphane Sabourau

DYCK'S SURFACES, SYSTOLES, AND CAPACITIES

MIKHAIL G. KATZ AND STÉPHANE SABOURAU

Abstract. We prove an optimal systolic inequality for nonpositively curved Dyck's surfaces. The extremal surface is flat with eight conical singularities, six of angle ϑ and two of angle $9\pi - 3\vartheta$ for a suitable ϑ with $\cos(\vartheta) \in \mathbb{Q}(\sqrt{19})$. Relying on some delicate capacity estimates, we also show that the extremal surface is not conformally equivalent to the hyperbolic Dyck's surface with maximal systole, yielding a first example of systolic extremality with this behavior.

Contents

2010 *Mathematics Subject Classification.* Primary 53C23; Secondary 30F10, 58J60 .

Key words and phrases. Systole, optimal systolic inequality, extremal metric, nonpositively curved surface, Riemann surface, Dyck's surface, hyperellipticity, antiholomorphic involution, conformal structure, capacity.

1. Introduction

The systole of a metric space M is the least length of a loop in M which cannot be contracted to a point. Only a small number of optimal systolic inequalities relating the systole and the volume of M are available in the literature. Loewner's torus inequality asserts that every Riemannian torus $\mathbb{T}$ satisfies

$$\operatorname{sys}(\mathbb{T}^2)^2 \leq \frac{2}{\sqrt{3}} \operatorname{area}(\mathbb{T}^2); \tag{1.1}$$

see Pu's paper [25]. Pu's inequality asserts that every real projective plane $\mathbb{RP}^2$ satisfies

$$\operatorname{sys}(\mathbb{RP}^2)^2 \leq \frac{\pi}{2} \operatorname{area}(\mathbb{RP}^2). \tag{1.2}$$

Bavard's inequality [3] for the Klein bottle K is the bound

$$\operatorname{sys}(K)^2 \leq \frac{\pi}{2\sqrt{2}} \operatorname{area}(K). \tag{1.3}$$

The Burago-Ivanov-Gromov inequality relates the stable 1-systole of an n-torus to its volume:

$$\operatorname{stsys}_1(\mathbb{T}^n) \leq \sqrt{\gamma_n} \operatorname{vol}_n(\mathbb{T}^n)^{\frac{1}{n}}, \tag{1.4}$$

where γ_n is the Hermite constant; see Burago and Ivanov [8], [9], Gromov [15], and [18, p. 155].

Bangert et al. proved the following optimal inequality for orientable Riemannian n-manifolds M:

$$\operatorname{stsys}_1(M) \operatorname{sys}_{n-1}(M) \leq \gamma'_b \operatorname{vol}_n(M) \tag{1.5}$$

where $b = b_1(M)$ is the first Betti number, and γ'_b is the Bergé-Martinet constant; see Bangert et al. [1], [2], and [18, p. 135].

In the context of nonpositively curved metrics, we proved the following optimal inequality in [19]: every nonpositively curved genus two surface Σ_2 satisfies the bound

$$\operatorname{sys}(\Sigma_2)^2 \leq \tfrac{1}{3}(\sqrt{2}+1) \operatorname{area}(\Sigma_2). \tag{1.6}$$

Furthermore, the equality case is attained by a piecewise flat metric with 16 conical singularities of angle $\frac{9\pi}{4}$. Such a metric can be expressed by a conformal factor vanishing at the singular points, with respect to a smooth metric (e.g., the hyperbolic one) in the conformal class of

the Bolza surface. The latter is the surface possessing the maximal group of symmetries in genus 2. The *hyperbolic* metric on the Bolza surface had also been shown to have maximal systole in this genus by Jenni [17] and others. The combination of these two (old) results can be summarized as follows.

Theorem 1.1. *The systolically extremal surface of nonpositive curvature and the systolically extremal hyperbolic surface belong to the same conformal class, namely that of the Bolza surface.*

It turns out that such coincidence of conformal classes no longer holds in the case of Dyck's surface (see Theorem 1.3).

In the present article, we develop an analogous optimal systolic inequality for nonpositively curved metrics on Dyck's surface. Here Dyck's surface $3\mathbb{RP}^2$ is the nonorientable closed surface of Euler characteristic -1, homeomorphic to the connected sums

$$\begin{aligned} 3\mathbb{RP}^2 &= \mathbb{RP}^2\#\mathbb{RP}^2\#\mathbb{RP}^2 \\ &= \mathbb{RP}^2\#\mathbb{T}^2. \end{aligned}$$

By convention, a point on Dyck's surface will be referred to as a Weierstrass point if it is the image of a Weierstrass point of the orientable double cover.

Theorem 1.2. *Each nonpositively curved metric on Dyck's surface* $3\mathbb{RP}^2$ *satisfies the following optimal systolic inequality:*

$$\operatorname{sys}(3\mathbb{RP}^2)^2 \leq \frac{12}{12+(169-38\sqrt{19})^{\frac{1}{2}}}\ \operatorname{area}(3\mathbb{RP}^2). \tag{1.7}$$

Furthermore, the equality case is attained by a piecewise flat surface composed of a flat Möbius band and three identical symmetric nonregular flat hexagons centered at its Weierstrass points.

Observe that the optimal constant $\frac{1}{3}(\sqrt{2}+1) \simeq 0.80473$ in (1.6) is less than the one in (1.7), which is approximately 0.86745. This is consistent with the expected monotonicity of the systolic area as a function of the Euler characteristic. For general metrics, it is more difficult to obtain estimates for the systolic ratio, but in [20] we obtained a small improvement (for Dyck's surface) of a general estimate of Gromov's.

We will refer to the extremal surface as the *extremal nonpositively curved Dyck's surface* and denote it $\mathcal{D}_{\leq 0}$. We present two constructions of $\mathcal{D}_{\leq 0}$, one in Section 2 and the other in Section 6. Theorem 1.2 is proved in Section 7.

The hyperbolic Dyck's surface of maximal systole, denoted by $\mathcal{D}_{-1}$, was described by Parlier [24] and then by Gendulphe [14]. It has the

same symmetry group as the extremal nonpositively curved Dyck's surface. However, using some recent work of B. Muetzel [23], we show that they are not conformally equivalent.

Theorem 1.3. *The conformal types of the extremal nonpositively curved Dyck's surface $\mathcal{D}_{\leq 0}$ and the extremal hyperbolic Dyck's surface $\mathcal{D}_{-1}$ are distinct, and can be distinguished by the capacities of the associated annuli $\mathcal{A}_{\leq 0}$ and $\mathcal{A}_{-1}$ obtained by cutting open their orientable double covers:*

$$\operatorname{Cap} \mathcal{A}_{\leq 0} < 2.29 < \operatorname{Cap} \mathcal{A}_{-1}$$

(see Section 8 for the definitions of the annuli).

This yields a first example of systolic extremality with this behavior, in contrast with the situation in genus 2 summarized in Theorem 1.1. In genus 3, the question is open.

Question 1.4. For genus 3 surfaces, do the extremal hyperbolic surface and the extremal surface of nonpositive curvature belong to the same conformal type?

We also observe that the orientable double cover of $\mathcal{D}_{\leq 0}$ is not conformally equivalent to the Bolza surface; *cf.* Proposition 8.1.

Since the extremal hyperbolic metric and the extremal singular flat metric on Dyck's surface are defined explicitly, one might have hoped to find a (simpler) indirect proof of the fact that they belong to distinct conformal classes. However, this appears to be difficult. We have therefore relied on the capacity estimate which produces a direct numerical argument distinguishing between the two conformal classes.

The proof of the main theorem makes use of an averaging argument by the hyperelliptic involution and the Rauch comparison theorem as in [19]. Unlike the situation treated in [19], the orientable double cover of the extremal surface does not have a maximal group of symmetries. Therefore our approach requires some new features. More specifically, it relies on the following:

(1) an analysis of the lengths of some distance curves to a canonical nonorientable loop;
(2) an analysis of some optimal flat pieces (hexagons and cylinder) of a partition of the extremal surface;
(3) a study of the combinatorics of these pieces;
(4) a delicate capacity estimate as explained above.

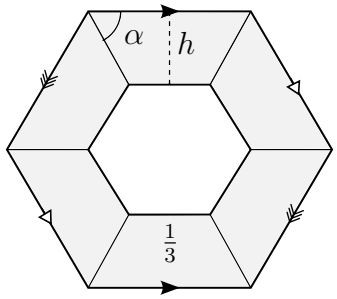

FIGURE 2.1. The hexagonal annulus $\mathcal{H}$

2. Description of the extremal surface

2.1. **Construction of the extremal surface.** In addition to the description below, we will present an alternative construction of the extremal surface at the end Section 6. We normalize the systole to 1. Consider real numbers α and h specified by the relations

$$\begin{cases} \alpha &= \frac{1}{2}\left(\pi - \arctan\sqrt{\frac{8-\sqrt{19}}{2}}\right) > \frac{\pi}{3} \\ h &= \frac{1}{2}\cos\alpha \end{cases} \tag{2.1}$$

The piecewise flat surface defining the extremal nonpositively curved Dyck's surface $\mathcal{D}_{\leq 0}$ can be constructed as follows.

(1) Take a flat isosceles trapezoid of height h and acute angle α with the shorter (internal) side of length $\frac{1}{3}$, where parameters α and h satisfy the relations (2.1);
(2) Form a nonplanar hexagonal annulus $\mathcal{H}$ composed of six identical trapezoids (see Figure 2.1), where the inner boundary component of $\mathcal{H}$ is of length 2;
(3) Form the torus with a disk removed, obtained from the hexagonal annulus $\mathcal{H}$ by identifying the opposite sides of the outer boundary component of the annulus, as in Figure 2.1;
(4) Attach a flat Möbius band of width $1-2h$ and boundary length 2 to the torus with a disk removed constructed in step (3).

The values of the parameter α and h are chosen so that the contribution of the hexagonal annulus and the Möbius band to the (systolic) area of the Dyck's surface is minimal. This optimal configuration forces the systolic loops to decompose into three families, *cf.* §2.5.

2.2. **Conical singularities.** The extremal surface $\mathcal{D}_{\leq 0}$ so defined is of nonpositive curvature in the sense of Alexandrov, since $6\alpha > 2\pi$. More precisely, it is piecewise flat and has eight conical singularities:

- two of angle 6α corresponding to the vertices of the outer boundary component of $\mathcal{H}$, and
- six of angle $3\pi - 2\alpha$ corresponding to the vertices of the inner boundary component of $\mathcal{H}$.

The angle ϑ of six of the eight conical singularities satisfies $\vartheta = 3\pi - 2\alpha$, which leads to the following expression:

$$\cos\vartheta = \frac{1+\sqrt{19}}{9} \in \mathbb{Q}(\sqrt{19}). \tag{2.2}$$

2.3. **Weierstrass points.** The Weierstrass points of $\mathcal{D}_{\leq 0}$ correspond to the midpoints of the sides of the outer boundary component of $\mathcal{H}$ after completion of the steps (1) through (4) of the construction of the extremal surface. The Weierstrass points of the extremal surface are actually smooth, therefore the quotient metric on S^2 from (3.4) has conical singularities of angle π at the six branch points, in addition to the singular points arising from the extremal metric.

The optimal configuration for $\mathcal{D}_{\leq 0}$ follows from an equilibrium between the systolic area contribution of the Möbius band and that of the Voronoi cells centered at the Weierstrass points.

2.4. **Automorphism groups.** The following proposition provides a description of the automorphism and symmetry groups of $\mathcal{D}_{\leq 0}$ viewed as a Riemannian Klein surface.

Proposition 2.1. *The automorphism group and the symmetry group of $\mathcal{D}_{\leq 0}$ are both isomorphic to*

$$D_3 \times \mathbb{Z}/2\mathbb{Z}.$$

Proof. The natural homomorphism between the automorphism (resp. symmetry) group of $\mathcal{D}_{\leq 0}$ and the permutation group D_3 of its Weierstrass points is surjective. Its kernel is composed of dianalytic (*i.e.* locally holomorphic or antiholomorphic) automorphisms preserving the Weierstrass points. The only two automorphisms with this property are the identity map and the hyperelliptic involution (which is an isometry). Since they commute with every holomorphic map (and so every isometry), *cf.* [13, §III.9], we deduce that the automorphism (resp. symmetry) group of $\mathcal{D}_{\leq 0}$ is isomorphic to $D_3 \times \mathbb{Z}/2\mathbb{Z}$. □

2.5. **Systolic loops.** There are three types of systolic loops on the extremal surface:

- the soul of the flat Möbius band,
- the loops orthogonal to a short base of one of the trapezoids of $\mathcal{H}$,
- the loops orthogonal to a leg of one of the trapezoids of $\mathcal{H}$.

Note that the last type of systolic loops contains loops joining any pair of Weierstrass points.

2.6. **Extremality.** Since the extremal surface admits regions at every point of which exactly one systolic loop passes, it is not extremal for the curvature-free systolic inequality on $3\mathbb{RP}^2$; *cf.* [12, Lemma 2.1]. Actually, a direct application of the characterization of conformally extremal surfaces established by Bavard in [4] shows that $\mathcal{D}_{\leq 0}$ is not even extremal in its conformal class for the curvature-free systolic inequality. Thus, an extremal metric for the curvature-free systolic inequality on $3\mathbb{RP}^2$ necessarily admits regions of both positive and negative curvature.

3. Conformal data

In this section, we review some conformal constructions and results that we will need for the proofs of Theorem 1.2 and Theorem 1.3. A Riemann surface homeomorphic to $3\mathbb{RP}^2$ is the quotient $3\mathbb{RP}^2 = \Sigma_2/\tau$ of a genus two Riemann surface Σ_2 by a fixed point-free antiholomorphic involution τ. Recall that every genus two Riemann surface Σ_2 is hyperelliptic. It admits an affine model

$$y^2 = p(x) \tag{3.1}$$

in $\mathbb{C}^2$, where p is a degree 6 complex polynomial with six distinct roots, which correspond to the Weierstrass points of Σ_2. In this presentation, the hyperelliptic involution

$$J : \Sigma_2 \to \Sigma_2$$

is given by the transformation $(x, y) \mapsto (x, -y)$ on the affine model. It is the only holomorphic involution of Σ_2 with six fixed points (which are the six Weierstrass points). By uniqueness, every holomorphic or antiholomorphic involution of Σ_2 commutes with J; *cf.* [13, §III.9]. In particular,

$$\tau \circ J = J \circ \tau. \tag{3.2}$$

Thus, the hyperelliptic involution J on Σ_2 descends to an involution, denoted $J_{\mathcal{D}}$, on $3\mathbb{RP}^2$:

$$J_{\mathcal{D}} : 3\mathbb{RP}^2 \to 3\mathbb{RP}^2. \tag{3.3}$$

The projection of the locus of the equation (3.1) to the x-coordinate induces a holomorphic double cover

$$Q : \Sigma_2 \to \mathbb{CP}^1 \tag{3.4}$$

ramified at the Weierstrass points of Σ_2. The presence of the real structure τ entails that the polynomial p in (3.1) may be assumed to have real coefficients, and that the involution $\tau : \Sigma_2 \to \Sigma_2$ restricts to the complex conjugation on the affine model, namely

$$\tau(x, y) = (\bar{x}, \bar{y}).$$

Since the upperhalf plane in $\mathbb{C}$ is a fundamental domain for the action of the complex conjugation, the points on $3\mathbb{RP}^2 = \Sigma_2/\tau$ can be represented by points in the closure of the upperhalf plane. More precisely, consider the northern hemisphere

$$\hat{\mathbb{C}}^+ \subset \mathbb{CP}^1 = \mathbb{C} \cup \{\infty\} = S^2,$$

with the equator included. We will think of the surface $3\mathbb{RP}^2$ as the ramified double cover

$$3\mathbb{RP}^2 \to \hat{\mathbb{C}}^+ \tag{3.5}$$

induced by (3.4). Such a cover is branched along the equator of the hemisphere $\hat{\mathbb{C}}^+$ as well as at three additional branch points, namely the projections to $\hat{\mathbb{C}}^+$ of the Weierstrass points of Σ_2.

Definition 3.1. Let $Y \subset \Sigma_2$ be the preimage of the northern hemisphere $\hat{\mathbb{C}}^+$ under the double cover Q of (3.4).

Clearly, Y is a torus with an open disk removed.

Let τ_∂ be the restriction of the involution τ of Σ_2 to the boundary circle ∂Y. The map τ_∂ is the antipodal map on the boundary circle ∂Y. The original surface $3\mathbb{RP}^2$ can be viewed as the quotient space of Y by τ_∂:

$$Y \to 3\mathbb{RP}^2 = Y/\tau_\partial. \tag{3.6}$$

By construction, the subsurface $Y \subset \Sigma_2$ is J-invariant and its boundary ∂Y is the fixed point set of the involution $J \circ \tau$ of (3.2) on Σ_2.

4. Area lower bound for some collars

We will reduce the problem to symmetric metrics, and then establish an optimal lower bound for the area of some collars in $3\mathbb{RP}^2$. Similar considerations for general metrics, albeit with worse constants, can be found in [20].

Definition 4.1. The average metric $\bar{g}$ of a Riemannian metric g on $3\mathbb{RP}^2$ by the hyperelliptic involution (3.3) is defined as

$$\bar{g} = \frac{g + J_{\mathcal{D}}^*(g)}{2}.$$

We will need the following results regarding the average metric.

Lemma 4.2 ([19], Lemma 4.2)**.** *The average metric $\bar{g}$ of a nonpositively curved Riemannian metric g on $3\mathbb{RP}^2$ is similarly nonpositively curved.*

Lemma 4.3 ([18])**.** *Let g be a Riemannian metric on $3\mathbb{RP}^2$. The average metric $\bar{g}$ has a better systolic area than g, that is,*

$$\frac{\operatorname{area}(\bar{g})}{\operatorname{sys}(\bar{g})^2} \leq \frac{\operatorname{area}(g)}{\operatorname{sys}(g)^2}.$$

By Lemmas 4.2 and 4.3, the nonpositively curved metric on $3\mathbb{RP}^2$ (and so its lift to $\Sigma = \Sigma_2$) may be assumed invariant under the hyperelliptic involution. We normalize the metric by rescaling it to unit systole, so that $\operatorname{sys}(3\mathbb{RP}^2) = 1$. These assumptions on the metric will be implicit throughout the article.

Consider the surface $Y \subset \Sigma$ as in Definition 3.1. Recall that Y is a torus with an open disk removed. Here, Y is endowed with the J- and τ-invariant nonpositively curved metric inherited from Σ. As the fixed-point set of the isometric involution $J \circ \tau$, the boundary ∂Y of Y is geodesic.

Lemma 4.4. *Relative to the normalisation $\operatorname{sys}(3\mathbb{RP}^2) = 1$, the level curves of Y at distance less than $\frac{1}{2}$ from ∂Y are loops freely homotopic to ∂Y. Furthermore, they are of length at least 2.*

Proof. By Morse theory, the level curve at distance r from ∂Y deforms to ∂Y if the function $f(p) = \operatorname{dist}(p, \partial Y)$ has no singular value between 0 and r. Let r be the least value for which this is not the case.

Since Y is nonpositively curved, there exist two length-minimizing paths of length r joining ∂Y to the same critical point of f on $f^{-1}(r)$. Furthermore, these two length-minimizing paths form a geodesic arc γ with endpoints in ∂Y which induces a nontrivial class in $\pi_1(Y, \partial Y)$. Note that γ orthogonally meets ∂Y at its endpoints.

Now, the hyperelliptic involution J on Y induces the homomorphism $-id$ on $\pi_1(Y, \partial Y)$. Thus, the arcs γ and $-J\gamma$ lie in the same relative homotopy class in $\pi_1(Y, \partial Y)$. From the flat strip theorem, these two geodesic arcs are parallel and bound with some arcs of ∂Y

a J-invariant flat rectangle. The center x of this rectangle is clearly a Weierstrass point and

$$\operatorname{length}\gamma = 2r = 2\operatorname{dist}(x, \partial Y). \tag{4.1}$$

Now, the segment joining ∂Y to x forms with its image by J a geodesic arc c with opposite endpoints on ∂Y. This arc c projects to a noncontractible loop of $3\mathbb{RP}^2$. Hence the length of c, which is twice $\operatorname{dist}(x, \partial Y)$, is at least 1. Combined with (4.1), we derive the first part of the lemma, namely

$$r \geq \frac{1}{2}.$$

Each of the two arcs of ∂Y joining a pair of opposite points projects to a noncontractible loop of $3\mathbb{RP}^2$. Therefore, the length of ∂Y is at least 2. Since Y is nonpositively curved and ∂Y is a closed geodesic, every loop of Y freely homotopic to ∂Y is of length at least 2, and so are the level curves of Y at distance less than r from ∂Y. □

The coarea inequality yields a first lower bound on the systolic area of a nonpositively curved metric on $3\mathbb{RP}^2$.

Proposition 4.5. *Consider a normalized nonpositively curved metric on $3\mathbb{RP}^2 = Y/\tau_\partial$ invariant by the hyperelliptic involution and let $\delta \in (0, \frac{1}{2})$. The δ-tubular neighborhood U_δ of ∂Y in Y is a topological cylinder which satisfies*

$$\operatorname{area}(U_\delta) \geq 2\delta.$$

In particular,

$$\operatorname{sys}(3\mathbb{RP}^2)^2 \leq \operatorname{area}(3\mathbb{RP}^2). \tag{4.2}$$

5. Decomposition of nonpositively curved Dyck's surfaces

We introduce a decomposition of Dyck's surface leading to the description of the extremal metric in Section 6. This decomposition will also allow us to estimate the systolic area of nonpositively curved metrics.

The decomposition is motivated by the following observation. If the systolic inequality (4.2) were optimal, the extremal surface could be defined from a flat cylinder of circumference 2 and height $\frac{1}{2}$ by identifying pairs of opposite points on one of its boundary component (which leads to a Möbius band) and by gluing the other boundary component onto itself so as to obtain the right topological type for the surface. It turns out this is impossible without decreasing the systole, which shows that the inequality (4.2) is not optimal.

Actually, we will see that the extremal surface decomposes into a flat Möbius band and a torus with a disk removed. The flat Möbius band is defined as previously from a flat cylinder of circumference 2 and height $\delta < \frac{1}{2}$, while the torus with a disk removed is made of three isometric flat hexagons.

The conical singularities will correspond to the points where the various flat regions meet. The sizes of the cylinder and the hexagons must be chosen to make the gluing possible while minimizing the systolic area. The comparison with nonpositively curved metrics will be carried out afterwards.

Let us introduce some quantities related to the sizes of the cylinder and hexagons, whose geometric interpretations will appear in Proposition 6.2.

Fix $h > 0$ and $\theta \in (0, \frac{\pi}{2})$ such that

$$\begin{cases} 2h &= \sin\frac{\theta}{2} \\ 6h &= \tan\theta \end{cases} \tag{5.1}$$

Note that

$$\tan\frac{\theta}{2} = \frac{2h}{\sqrt{1-4h^2}}. \tag{5.2}$$

More explicitly, we have

$$\begin{cases} h &= \sqrt{\frac{8-\sqrt{19}}{72}} \simeq 0.2248796 \\ \theta &= \arctan\sqrt{\frac{8-\sqrt{19}}{2}} < \frac{\pi}{3} \end{cases} \tag{5.3}$$

Let $\delta \in (0, \frac{1}{2})$ be defined as $\delta = \frac{1}{2} - h$.

We will use the notations and assumptions from the previous section. In particular, we assume that $3\mathbb{RP}^2 = Y/\tau_\partial$ as in (3.6) is endowed with a normalized nonpositively curved metric invariant under the hyperelliptic involution (3.3). We would like to decompose Y into U_δ and three Voronoi cells centered at the three Weierstrass points of Y. The main theorem will then follow from a comparison between the areas of these Voronoi cells and those of some Euclidean polygons. In order to describe the Voronoi cells and their comparison Euclidean polygons, it is convenient to proceed as follows.

Since Σ is nonpositively curved, the open collar C_δ of width δ around the closed geodesic ∂Y of Σ is convex. Removing this collar and gluing back the boundary components of $\Sigma \setminus C_\delta$ yields a new CAT(0) genus two surface Σ_0. We will identify the regions of Σ_0 with those of $\Sigma \setminus C_\delta$.

Let $\tilde{\Sigma}_0$ be the universal cover of Σ_0. The Voronoi cell of $\tilde{\Sigma}_0$ centered at a lift of a Weierstrass point of Σ_0 is the region of $\tilde{\Sigma}_0$ formed of the points closer to this lift than to any other lift of a Weierstrass point. The Voronoi cells on $\tilde{\Sigma}_0$ are polygons whose edges are arcs of the equidistant curves between a pair of lifts of Weierstrass points. Note that these edges are not necessarily geodesics. Since the metric is nonpositively curved, the Voronoi cells on $\tilde{\Sigma}_0$ are topological disks, while their projections to Σ or $3\mathbb{RP}^2$, still called Voronoi cells, may have more complicated topology. Note that the Voronoi cells on $\tilde{\Sigma}_0$ have the same area as their projections to Σ or $3\mathbb{RP}^2$. This is because the *interior* of a Voronoi cell projects injectively.

Furthermore, since the metric on Σ_0 is J-invariant, the Voronoi cells on $\tilde{\Sigma}_0$ are symmetric with respect to their centers, and since it is also $(J \circ \tau)$-invariant, the projections of their boundaries to Σ contain the boundary components of C_δ.

Now assume $y \in \tilde{\Sigma}_0$ is the lift of a Weierstrass point, and let $y' \in \tilde{\Sigma}_0$ be the lift of another Weierstrass point. Denote by $x' \in T_y$ the preimage of y' by the exponential map $\exp_y$ from the tangent plane T_y to $\tilde{\Sigma}_0$ at y. Define $L_{x'}$ as the equidistant line in T_y between the origin $x \in T_y$ and x'. For every $x'' \in L_{x'}$, set $y'' = \exp_y(x'')$. By the Rauch comparison theorem, the exponential map $\exp_y$ does not decrease distances. Thus,

$$\mathrm{dist}_{\tilde{\Sigma}_0}(y, y'') = \mathrm{dist}_{T_y}(x, x'') = \mathrm{dist}_{T_y}(x', x'') \leq \mathrm{dist}_{\tilde{\Sigma}_0}(y', y''). \quad (5.4)$$

Consider the Euclidean polygon in the tangent plane T_y, obtained as the intersection of the halfspaces containing the origin, defined by the lines $L_{x'}$, as y' runs over all Weierstrass points distinct from y. This Euclidean polygon will be referred to as the *comparison Euclidean polygon* corresponding to the Voronoi cell centered at y. It follows from the inequality (5.4) that the exponential image of this polygon is contained in the Voronoi cell of y. Since the exponential map does not decrease distances, we obtain the following proposition.

Proposition 5.1. *The area of a Voronoi cell is bounded from below by the area of its comparison Euclidean polygon.*

By construction, Y decomposes into U_δ and three Voronoi cells centered at the three Weierstrass points of Y.

We conclude this section with some distance estimates on the centers of the Voronoi cells of Y, that is, on the Weierstrass points.

Lemma 5.2.

(1) *The distance between two Weierstrass points of Y is at least $\frac{1}{2}$.*
(2) *Every Weierstrass point of Y is at distance at least h from U_δ.*

Proof. Every minimizing segment between a pair of isolated branch points of the double cover $3\mathbb{RP}^2 \to \hat{\mathbb{C}}^+$ lifts to a noncontractible loop of $3\mathbb{RP}^2$. Thus, the distance between two Weierstrass points of Y is at least $\frac{1}{2}$. Similarly, every minimizing segment between an isolated branch point of $3\mathbb{RP}^2 \to \hat{\mathbb{C}}^+$ and the equator lifts to a noncontractible loop of $3\mathbb{RP}^2$. Thus, every Weierstrass point of Y is at distance at least $\frac{1}{2}$ from ∂Y and so at distance at least h from U_δ. □

6. The extremal nonpositively curved Dyck's surface

In this section, we bound from below the area of the Voronoi cells in some special case and describe the extremal nonpositively curved Dyck's surface using the constructions and notation defined earlier.

As previously, we assume that $3\mathbb{RP}^2$ is endowed with a normalized nonpositively curved metric invariant under the hyperelliptic involution. This metric descends to a singular metric on $\hat{\mathbb{C}}^+$ under the ramified cover (3.5).

Definition 6.1. Let Γ on $\hat{\mathbb{C}}^+$ be the connected graph given by the projections of the edges of the Voronoi cells to the hemisphere, see Proposition 5.1. Denote by $\hat{\mathbb{C}}^+_\delta$ the spherical cap of $\hat{\mathbb{C}}^+$ bounded by the level curve c_δ of $\hat{\mathbb{C}}^+$ at distance δ from the equator. From Lemma 4.4, the length of c_δ is at least 1.

By construction, the graph Γ lies in $\hat{\mathbb{C}}^+_\delta$, contains c_δ and bounds $f = 3$ faces. From the formula $v - e + f = 1$, where v and e are the numbers of vertices and edges of Γ, and the well-known inequality $3v \leq 2e$, we derive that Γ has at most 6 edges and 4 vertices.

Suppose that Γ has three vertices lying in c_δ and a fourth one in the interior of $\hat{\mathbb{C}}^+_\delta$ from which arise three edges connecting the three other vertices on c_δ, *cf.* Figure 6.1. In other words, Γ bounds three triangles in $\hat{\mathbb{C}}^+_\delta$.

By construction, each of these triangles lifts to a hexagonal Voronoi cell in $\tilde{\Sigma}_0$ whose comparison Euclidean polygon is a (symmetric) hexagon. Furthermore, the center of this Euclidean hexagon H is at distance at least $\frac{1}{4}$ from two pairs of opposite sides and at distance at least h from the other pair of opposite sides, see Lemma 5.2.

The following result provides a sharp lower bound on the area of the comparison Euclidean hexagon and therefore on the hexagonal Voronoi cells.

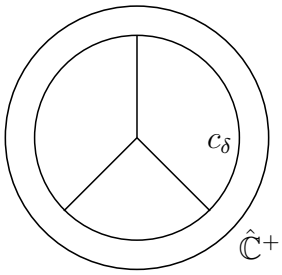

FIGURE 6.1. Triangular decomposition of $\hat{\mathbb{C}}^+_\delta$

Proposition 6.2. *Let H be the symmetric Euclidean hexagon which is the comparison hexagon of the Voronoi cell as above. Then*

$$\mathrm{area}(H) \geq h\sqrt{1-4h^2}.$$

Furthermore, the equality case is attained by a symmetric Euclidean hexagon composed of six pairwise opposite isosceles triangles based at its center: four of them have height $\frac{1}{4}$ and main angle θ, and two of them have height h and base $\frac{1}{3}$, cf. Figure 6.2. Here, h and θ are defined in (5.1).

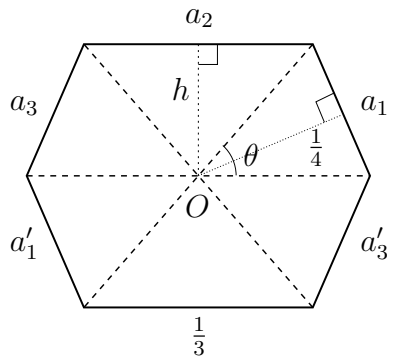

FIGURE 6.2. The hexagon H

Remark 6.3. Note that the angles between two sides of length other than $\frac{1}{3}$ are equal to $\pi - \theta > \frac{2\pi}{3}$.

Proof of Proposition 6.2. Let O be the center of H. Denote by a_1, a_2, a_3, a_1', a_2' and a_3' the sides of H (in this order) with a_i' opposite to a_i such that $d(O,a_1) \geq \frac{1}{4}$, $d(O,a_2) \geq h$ and $d(O,a_3) \geq \frac{1}{4}$, *cf.* Figure 6.2. The area of the triangle T_i with vertex O and side a_i is bounded from below by

$$d(O,a_i)^2 \tan\frac{\alpha_i}{2},$$

where α_i is the angle of T_i at O. Thus, from the relation $\alpha_1 + \alpha_2 + \alpha_3 = \pi$, we have

$$\begin{aligned} \operatorname{area} H &\geq 2\left(\frac{1}{4}\right)^2 \tan\frac{\alpha_1}{2} + 2\,h^2 \tan\frac{\alpha_2}{2} + 2\left(\frac{1}{4}\right)^2 \tan\frac{\alpha_3}{2} \\ &\geq 4\left(\frac{1}{4}\right)^2 \tan\frac{\alpha}{2} + 2\,\frac{h^2}{\tan\alpha}, \end{aligned}$$

where $\alpha = \frac{\alpha_1+\alpha_3}{2}$. The second inequality comes from the definition of convexity applied to the convex function $\tan(x/2)$ between α_1 and α_3. Using a classical relation between $\tan(\alpha)$ and $\tan(\alpha/2)$, we observe that this lower bound is minimal when

$$\tan^2\frac{\alpha}{2} = \frac{4h^2}{1-4h^2},$$

that is, when $\alpha = \theta$ from (5.2). The minimal lower bound is

$$h\sqrt{1-4h^2}. \tag{6.1}$$

Furthermore, the equality case occurs only if T_1 and T_3 are isosceles triangles of height $\frac{1}{2}$ and main angle θ, and T_2 is an isosceles triangle of height h and main angle $\pi - 2\theta$. From our choice of h and θ, *cf.* (5.1), the sides arising from the main vertices of these isosceles triangles have the same length, namely

$$\frac{1/4}{\cos\frac{\theta}{2}} = \frac{h}{\sin\theta}.$$

This shows that it is possible to put these isosceles triangles together in order to obtain an hexagon satisfying the desired constraints with area (6.1). In this case, the base of T_2 is of length

$$2\,\frac{h}{\tan\theta} = \frac{1}{3}.$$

□

From Proposition 4.5 and Proposition 6.2, the nonpositively curved Dyck's surface $3\mathbb{RP}^2$, which decomposes into the δ-tubular neighborhood U_δ and three hexagonal Voronoi cells, satisfies the following area lower bound

$$\begin{aligned} \operatorname{area}(3\mathbb{RP}^2) &\geq 2\delta + 3h\sqrt{1-4h^2} \\ &\geq 1 + \frac{1}{12}\sqrt{169 - 38\sqrt{19}} \end{aligned} \tag{6.2}$$

This area lower bound is optimal. It is attained by the nonpositively curved (in Alexandrov's sense) piecewise flat Dyck's surface $\mathcal{D}_{\leq 0}$

obtained as follows. Glue three copies of the optimal flat hexagon described in Proposition 6.2 and identify the opposite sides of lengths other than $\frac{1}{3}$, *cf.* Figure 6.3 and Remark 6.3.

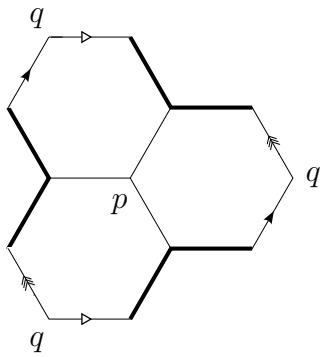

FIGURE 6.3. Three hexagonal Voronoi cells

The resulting surface is of boundary length 2. Now attach a flat cylinder of circumference 2 and height δ to it and identify the opposite boundary points. We obtain a nonpositively curved (in Alexandrov's sense) piecewise flat Dyck's surface $\mathcal{D}_{\leq 0}$ with two conical singularities p and q of angle $3(\pi-\theta) > 2\pi$ where the three hexagons meet, and six conical singularities of angle $2\pi+\theta$ at the other vertices of the hexagons.

Its area satisfies

$$\operatorname{area} \mathcal{D}_{\leq 0} = 1 + \frac{1}{12}\sqrt{169 - 38\sqrt{19}} \simeq 1.15279. \tag{6.3}$$

Proposition 6.4. *The surface $\mathcal{D}_{\leq 0}$ has unit systole.*

Proof. By construction, the extremal surface $\mathcal{D}_{\leq 0}$ decomposes into an open flat Möbius band $\mathcal{M}$ and six trapezoids; *cf.* Section 2. The Möbius band has unit systole. Hence, the systole of $\mathcal{D}_{\leq 0}$ is at most 1. Furthermore, every geodesic arc of $\mathcal{M}$ with endpoints on $\partial\mathcal{M}$ is of length at least $2\delta = 1 - 2h$. Similarly, every geodesic arc of the complement

$$\mathcal{D}_{\leq 0} \setminus \mathcal{M}$$

with endpoints on $\partial\mathcal{M}$ is of length at least $2h$. Thus, a noncontractible geodesic loop of $\mathcal{D}_{\leq 0}$ intersecting $\mathcal{M}$ is of length at least 1.

Consider now a systolic loop γ of $\mathcal{D}_{\leq 0}$ which does not meet $\mathcal{M}$. Denote by c its projection to $\hat{\mathbb{C}}^+$ by the ramified cover (3.5). By construction, the loop c lies in the spherical cap $\hat{\mathbb{C}}^+_\delta$ of $\hat{\mathbb{C}}^+$, *cf.* Definition 6.1. Here, the hemisphere $\hat{\mathbb{C}}^+$ is endowed with the quotient metric from $\mathcal{D}_{\leq 0}$. Furthermore, the loop c surrounds more than one branch point in $\hat{\mathbb{C}}^+$, otherwise its lift γ would be contractible in $\mathcal{D}_{\leq 0}$.

Suppose that c is not simple. Every arc of c forming a simple loop surrounds exactly one branch point of (3.5) in $\hat{\mathbb{C}}^+$. Indeed, if it surrounded exactly two branch points, it would lift to a noncontractible loop of $\mathcal{D}_{\leq 0}$ shorter than γ, which is impossible. If it surrounded three branch points, it would be double covered by a loop of $\mathcal{D}_{\leq 0} \setminus \mathcal{M}$ homotopic to $\partial\mathcal{M}$ and so of length at least 1, which is impossible since the systole of $\mathcal{D}_{\leq 0}$ is at most 1. Now, since c surrounds more than one branch point, there exist two arcs of c forming two simple loops surrounding two different branch points. From these two simple loops, we can form with the shorter path of c joining them a loop in $\hat{\mathbb{C}}^+$ homotopic to a simple loop surrounding exactly two branch points. By smoothing out its corners, the loop we just formed can be made shorter than c. This yields a contradiction as it lifts to a noncontractible loop of $\mathcal{D}_{\leq 0}$.

In conclusion, the loop c is simple and surrounds at least two branch points. Now, if it surrounds three branch points, we already showed that it is of length at least 1. If it surrounds exactly two branch points, its lift γ is homotopic to one of the three geodesic loops of length 1 made of the two segments connecting a pair of Weierstrass points. In this case, the length of γ is also equal to 1 since the metric is nonpositively curved. □

7. Other decompositions are not optimal

In this section, we complete the proof of Theorem 1.2 by showing that the other configurations for Γ, *cf.* Definition 6.1, correspond to nonpositively curved Dyck's surfaces with larger area.

We start with some area estimates on the Voronoi cells of a nonpositively curved Dyck's surface $3\mathbb{RP}^2$ with unit systole, whose metric is invariant by its hyperelliptic involution.

Lemma 7.1. *Every Voronoi cell of* $3\mathbb{RP}^2$ *has area at least*

$$\pi h^2 \simeq 0.15887.$$

Proof. From Lemma 5.2, the centers of the Voronoi cells are at distance at least $\frac{1}{2}$ from each other. In particular, every Voronoi cell contains an embedded disk of radius $h < \frac{1}{4}$. Since the metric is nonpositively curved the area of this disk is at least πh^2. □

Lemma 7.2. *A Voronoi cell of* $3\mathbb{RP}^2$ *whose projection to* $\hat{\mathbb{C}}^+$ *has an edge of length* x *lying in* c_δ *has area at least* $2hx$.

Proof. The comparison Euclidean polygon of such a Voronoi cell is a convex polygon of $\mathbb{R}^2$, symmetric with respect to its center O, with two opposite sides of length x at distance at least h from O. These two opposite sides span a parallelogram lying in the Euclidean polygon, which clearly satisfies the desired area lower bound. □

Lemma 7.3. *A Voronoi cell of* $3\mathbb{RP}^2$ *whose projection to* $\hat{\mathbb{C}}^+$ *is bounded by exactly two edges has area at least* h*.*

Proof. The comparison Euclidean polygon of such a Voronoi cell has four sides. It is a parallelogram with two opposite sides at distance at least $2h$ from each other; the other two sides are at distance at least 1 from each other. Hence its area is at least h. □

Recall that the graph Γ (see Section 6, Definition 6.1) has at most four vertices. Clearly, the valence of each vertex is at least 3 and at least one of the vertices lies in c_δ. We will consider four cases based on the number of vertices lying in c_δ.

Before starting our discussion, we observe that a face of $\hat{\mathbb{C}}^+_\delta$ cannot be bounded by a single edge of Γ, otherwise its comparison Euclidean polygon would be bounded by two halfspaces, which is impossible. This observation and the restriction on the number of faces of $\hat{\mathbb{C}}^+_\delta$ will be implicitely used in the description of the different cases below.

Case 1: Suppose that only one vertex lies in c_δ. By assumption, there is a Voronoi cell of $3\mathbb{RP}^2$ whose projection to $\hat{\mathbb{C}}^+$ has c_δ as an edge. From Lemma 7.2, the area of this cell is at least

$$2h\,\mathrm{length}(c_\delta) \geq 2h.$$

Since the area of each of the other two cells of $3\mathbb{RP}^2$ is at least πh^2, *cf.* Lemma 7.1, we obtain using Proposition 4.5 that

$$\mathrm{area}(3\mathbb{RP}^2) \geq 2\delta + 2h + 2\pi h^2 = 1 + 2\pi h^2 > \mathrm{area}\,\mathcal{D}_{\leq 0}\,.$$

Case 2: Suppose that exactly two vertices lie in c_δ. The two edges of c_δ, of length x and y, are part of two different faces of $\hat{\mathbb{C}}^+_\delta$. From Lemma 7.2, the total area of the two corresponding Voronoi cells of $3\mathbb{RP}^2$ is at least $2hx + 2hy = 2h$. Since the area of the third cell of $3\mathbb{RP}^2$ is at least πh^2, *cf.* Lemma 7.1, we conclude using Proposition 4.5 that

$$\mathrm{area}(3\mathbb{RP}^2) \geq 2\delta + 2h + \pi h^2 = 1 + \pi h^2 > \mathrm{area}\,\mathcal{D}_{\leq 0}\,.$$

Case 3: Suppose that exactly three vertices lie in c_δ.

If a fourth vertex lies in the interior of $\hat{\mathbb{C}}^+_\delta$, then we are in the situation already described in Section 6.

If there is no fourth vertex, two faces of $\hat{\mathbb{C}}^+_\delta$ are bounded by exactly two edges. By Lemma 7.3, the total area of the two corresponding Voronoi cells in $3\mathbb{RP}^2$ is at least $2h$. We conclude as in Case 2.

Case 4: Suppose that four vertices lie in c_δ, which is the maximal number of vertices of Γ. In this case, two faces of $\hat{\mathbb{C}}^+_\delta$ are bounded by exactly two edges and we conclude as in Case 3.

This proves that the optimal systolic inequality for nonpositively curved Dyck's surfaces is given by (6.2), where the equality case is attained by the surface $\mathcal{D}_{\leq 0}$ described at the end of Section 6.

8. Conformal classes of extremal Dyck's surfaces

In this section, we compare the conformal classes of three genus two Riemann surfaces that are significant for various systolic extremality problems. More specifically, we consider the Bolza surface $\mathcal{B}$ and the two orientable double covers of the extremal hyperbolic Dyck's surface $\mathcal{D}_{-1}$ and the extremal nonpositively curved Dyck's surface $\mathcal{D}_{\leq 0}$.

8.1. **The Bolza and Dyck's surfaces.**

The following well-known result shows that the Bolza surface is not the orientable double cover of any Dyck's surface.

Proposition 8.1. *The Bolza surface $\mathcal{B}$ admits no fixed point-free antiholomorphic involution.*

Proof. Suppose there is a fixed point-free antiholomorphic involution τ on $\mathcal{B}$. Recall that τ commutes with the hyperelliptic involution J. Both quotients $S^2 = \mathcal{B}/J$ and $3\mathbb{RP}^2 = \mathcal{B}/\tau$ admit a ramified double cover over the hemisphere $\hat{\mathbb{C}}^+$, *cf.* Section 3. The boundary of $\hat{\mathbb{C}}^+$ is double covered by a loop of $\mathcal{B}$ on which both J and τ act as an antipodal map.

In the setting of Section 3, the projection of this loop to S^2 is an equator with no branch point lying in it. The quotient map $\bar{\tau} : S^2 \to S^2$ induced by τ is an anticonformal map which fixes pointwise the equator and switches the two hemispheres. Thus, the composition $\bar{\tau} \circ \varphi$ of $\bar{\tau}$ with the reflexion φ along the equator conformally acts on each hemisphere fixing pointwise the equator.

By applying the Cauchy integral formula to the holomorphic map $\bar{\tau} \circ \varphi$ on each hemisphere or simply by complex analytic continuation, we deduce that the composition $\bar{\tau} \circ \varphi$ is the identity map. Thus, the map $\bar{\tau}$ is the reflexion along this equator containing no branch point. Since $\bar{\tau}$ preserves the branch points of the ramified double cover $\mathcal{B} \to S^2$, we derive a contradiction. Indeed, the branch points of the Bolza surface

form a regular octahedron on S^2 and all the reflexions of S^2 acting on this octahedron fix at least one vertex, which is not the case of $\bar{\tau}$. $\square$

8.2. **Conformal collar and capacity.** We introduce a conformal invariant which will allow us to distinguish the conformal classes of the extremal nonpositively curved Dyck's surface $\mathcal{D}_{\leq 0}$ and the extremal hyperbolic Dyck's surface $\mathcal{D}_{-1}$.

Recall that the extremal hyperbolic Dyck's surface $\mathcal{D}_{-1}$ described in [24] and [14] is obtained by identifying opposite pairs of points on the boundary component of the maximal hyperbolic surface of signature $(1,1)$ with boundary length

$$\ell = 2\,\mathrm{arccosh}\left(\frac{5+\sqrt{17}}{2}\right) \simeq 4.397146,$$

cf. [27, p. 578]. The term "maximal" refers to a hyperbolic surface with fixed geodesic boundary length whose systole is maximal. The systole of the extremal hyperbolic Dyck's surface $\mathcal{D}_{-1}$ is equal to $\ell/2$. Furthermore, $\mathcal{D}_{-1}$ has the same isometry group G as $\mathcal{D}_{\leq 0}$, which is isomorphic to $D_3 \times \mathbb{Z}/2\mathbb{Z}$, *cf.* Proposition 2.1.

Definition 8.2. Consider a G-invariant conformal structure on Dyck's surface $3\mathbb{RP}^2$ (*e.g.*, the conformal structure of $\mathcal{D}_{\leq 0}$ or $\mathcal{D}_{-1}$). The union of the fixed-point sets of the order two automorphisms of $3\mathbb{RP}^2$ defines a graph. By removing the edges of this graph which meet the ramification locus of (3.5) at non-Weierstrass points, we obtain a graph Γ on $3\mathbb{RP}^2$. The *collar (or annulus) corresponding to the conformal structure of* $3\mathbb{RP}^2$ is the orientable double cover $\mathcal{A}$ of the surface obtained by cutting $3\mathbb{RP}^2$ open along Γ. By definition, it only depends on the conformal structure of the Dyck's surface.

For example, the graph Γ on the extremal nonnegatively curved Dyck's surface agrees with the outer boundary component of $\mathcal{H}$ after identification of the opposite sides, *cf.* Figure 2.1.

The *soul* of the open collar $\mathcal{A}$ is the simple loop C defined as the ramification locus of

$$\mathcal{A} \subset \Sigma^2 \to 3\mathbb{RP}^2 \to \hat{\mathbb{C}}^+$$

(since the collar is open the Weierstrass points are excluded), see (3.5).

Let us recall the following definition.

Definition 8.3. The *capacity* of a Riemannian collar $\mathcal{A}$, with boundary components $\partial\mathcal{A}_-$ and $\partial\mathcal{A}_+$, is defined as

$$\operatorname{Cap}\mathcal{A} = \inf_u \int_{\mathcal{A}} |\nabla u|^2 \tag{8.1}$$

where u runs over piecewise smooth functions on $\mathcal{A}$ with $u = 0$ on $\partial\mathcal{A}_-$ and $u = 1$ on $\partial\mathcal{A}_+$.

The infimum is attained by the unique harmonic function satisfying the boundary conditions. The capacity is a conformal invariant.

Remark 8.4. By construction, the capacity of the collar corresponding to a G-invariant conformal structure of $3\mathbb{RP}^2$ is a conformal invariant of the surface.

In the rest of the article, we estimate the collar capacities for the extremal nonpositively curved Dyck's surface $\mathcal{D}_{\leq 0}$ and the extremal hyperbolic Dyck's surface $\mathcal{D}_{-1}$

8.3. **Collar capacity for $\mathcal{D}_{\leq 0}$.** In the following proposition, we bound from above the capacity of the collar corresponding to the extremal nonpositively curved Dyck's surface.

Proposition 8.5. *Let $\mathcal{A}_{\leq 0}$ be the collar corresponding to the conformal structure of the extremal nonpositively curved Dyck's surface $\mathcal{D}_{\leq 0}$. Then*

$$\operatorname{Cap}\mathcal{A}_{\leq 0} \leq 2.28308.$$

Proof. The surface $\mathcal{D}_{\leq 0}$ is tiled by three flat "hexagons" (flat hexagons with two flat rectangles attached to them) centered at the Weierstrass points, *cf.* Figure 6.3. By construction, the collar $\mathcal{A}_{\leq 0}$ (composed of a cylinder and half hexagons) has piecewise geodesic boundary components.

The simple loop C decomposes the collar $\mathcal{A}_{\leq 0}$ into two regions $\mathcal{A}^+_{\leq 0}$ and $\mathcal{A}^-_{\leq 0}$. We define a piecewise smooth function u on $\mathcal{A}_{\leq 0}$ as follows

$$u(x) = \begin{cases} \min\{\frac{1}{2} + d(x, C), 1\} & \text{if } x \in \mathcal{A}^+_{\leq 0} \\ \\ \max\{\frac{1}{2} - d(x, C), 0\} & \text{if } x \in \mathcal{A}^-_{\leq 0} \end{cases}$$

Since the points on the boundary components of $\mathcal{A}_{\leq 0}$ are at distance at least $\frac{1}{2}$ from C, the function u is a test function for the capacity of $\mathcal{A}_{\leq 0}$, *cf.* (8.1). Thus,

$$\begin{aligned} \operatorname{Cap}\mathcal{A}_{\leq 0} &\leq \int_{\mathcal{A}_{\leq 0}} |\nabla u|^2 \\ &\leq \operatorname{area}\{x \in \mathcal{A}_{\leq 0} \mid d(x, C) \leq \frac{1}{2}\}. \end{aligned} \tag{8.2}$$

There is a unique minimizing ray r_x from every point x of $\mathcal{A}_{\leq 0}$ to C. The points x of $\mathcal{A}_{\leq 0}$ such that r_x passes through a given conical singularity x_0 form a symmetric flat quadrilateral Q_{x_0}, with two right angles from which two edges of length h meeting at x_0 with an angle θ arise, *cf.* Figure 8.1. Recall that the constants h and θ are defined in (5.3).

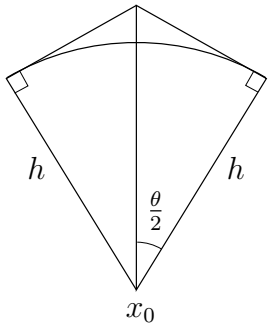

FIGURE 8.1. The quadrilateral Q_{x_0}

The points of Q_{x_0} outside the disk of radius h centered at x_0 are at distance at least $\frac{1}{2}$ from C. They form a region of area

$$\left[\tan\left(\frac{\theta}{2}\right) - \frac{\theta}{2}\right] h^2.$$

Furthermore, the quadrilaterals Q_{x_0} are disjoint as x_0 runs over the conical singularities of $\mathcal{A}_{\leq 0}$. Continuing with (8.2), we obtain the following upper bound for the capacity of $\mathcal{A}_{\leq 0}$ using (6.3)

$$\begin{aligned} \operatorname{Cap} \mathcal{A}_{\leq 0} &\leq 2 \operatorname{area} \mathcal{D}_{\leq 0} - 12 \left[\tan\left(\frac{\theta}{2}\right) - \frac{\theta}{2}\right] h^2 \\ &\leq 2.28308. \end{aligned}$$

□

8.4. **A general lower bound on the capacity of a collar.** We will need the following lower bound on the capacity of a collar. This bound was established by B. Muetzel [23, Lemma 2.2] in a more general form. We include a proof for the reader's convenience.

Lemma 8.6 (B. Muetzel)**.** *Consider a hyperbolic collar $\mathcal{A}$ around a closed geodesic loop of length ℓ parametrized in Fermi coordinates by*

$$\{(t, s) \mid t \in [0, \ell), s \in (a(t), b(t))\}.$$

Then

$$\operatorname{Cap} \mathcal{A} \geq \int_0^\ell \frac{1}{H(b(t)) - H(a(t))}\, dt$$

where $H(s) = 2 \arctan(\exp(s))$.

Proof. In Fermi coordinates, the hyperbolic metric on $\mathcal{A}$ can be expressed as $g = \cosh(s)^2\, dt^2 + ds^2$, *cf.* [10]. Let ξ be the unit vector field on $\mathcal{A}$ induced by $\frac{\partial}{\partial s}$. For every piecewise smooth function u on $\mathcal{A}$ with $u = 0$ on $\partial\mathcal{A}_-$ and $u = 1$ on $\partial\mathcal{A}_+$, we have

$$\int_{\mathcal{A}} |\nabla u|^2 \geq \int_{\mathcal{A}} g(\nabla u, \xi)^2 = \int_0^{\ell} \int_{a(t)}^{b(t)} \left(\frac{\partial u}{\partial s}\right)^2 \cosh(s)\, ds\, dt.$$

Given a continuous function $h : [a, b] \to (0, \infty)$ (in our case, $h(s) = \cosh(s)$), we want to minimize the integral

$$\int_a^b f'(s)^2\, h(s)\, ds$$

where $f : [a, b] \to \mathbb{R}$ is a piecewise smooth function with $f(a) = 0$ and $f(b) = 1$. Let H be a primitive of $\frac{1}{h}$. Making the change of variables $\tau = H(s)$, we obtain

$$\begin{aligned} \int_a^b f'(s)^2\, h(s)\, ds &= \int_{H(a)}^{H(b)} \left[f'(H^{-1}(\tau)) \cdot h(H^{-1}(\tau))\right]^2 d\tau \\ &= \int_{H(a)}^{H(b)} (f \circ H^{-1})'(\tau)^2\, d\tau \end{aligned} \tag{8.3}$$

since $(H^{-1})'(\tau) = h(H^{-1}(\tau))$. By the Cauchy-Schwarz inequality, we have

$$1 = \left(\int_{H(a)}^{H(b)} (f \circ H^{-1})'(\tau)\, d\tau\right)^2 \leq (H(b) - H(a)) \int_{H(a)}^{H(b)} (f \circ H^{-1})'(\tau)^2\, d\tau.$$

Hence,

$$\int_a^b f'(s)^2\, h(s)\, ds \geq \frac{1}{H(b) - H(a)}.$$

Therefore,

$$\int_{\mathcal{A}} |\nabla u|^2 \geq \int_0^{\ell} \frac{dt}{H(b(t)) - H(a(t))}.$$

□

8.5. **Collar capacity for $\mathcal{D}_{-1}$.** In the following proposition, we bound from below the capacity of the collar corresponding to the extremal hyperbolic Dyck's surface.

Proposition 8.7. *Let $\mathcal{A}_{-1}$ be the collar corresponding to the conformal structure of the extremal hyperbolic Dyck's surface $\mathcal{D}_{-1}$. Then*

$$\mathcal{A}_{-1} \geq 2.29461.$$

Proof. The surface $\mathcal{D}_{-1}$ is tiled by three hyperbolic hexagons centered at the Weierstrass points, *cf.* [14]. By construction, the collar $\mathcal{A}_{-1}$ is made of half hexagons with one side lying in C and has piecewise geodesic boundary components.

Each tiling hyperbolic hexagon of $\mathcal{D}_{-1}$ decomposes into four isometric trirectangles with an acute angle equal to $\frac{\pi}{3}$. The sides a and b opposite to the acute angle are of length $\ell/4$ and $\ell/12$, with the shorter side b lying in C. Observe that $\mathcal{A}_{-1}$ is composed of exactly 24 such trirectangles T. From the hyperbolic formula [10, p. 454, 2.3.1(iv)] for trirectangles, the geodesic arc of T orthogonal to b at the point at distance t from a, *cf.* Figure 8.2, is of length

$$\operatorname{arctanh}\left[\cosh(t)\,\tanh\left(\frac{\ell}{4}\right)\right]. \tag{8.4}$$

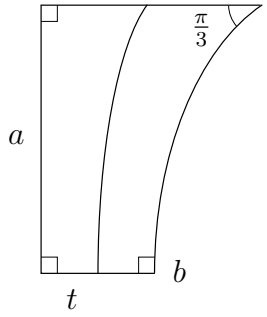

FIGURE 8.2. The trirectangle T

In Fermi coordinates, the collars $\mathcal{A}_{-1}$ is parametrized by

$$\{(t,s) \mid t \in [0,\ell), s \in (-a(t), a(t))\}$$

where $a(t)$ agrees with (8.4) for $t \in [0, \frac{\ell}{12})$ (the other values can be derived by symmetry). From Muetzel's Lemma 8.6, we have

$$\begin{aligned} \operatorname{Cap}\mathcal{A}_{-1} &\geq 12\int_0^{\frac{\ell}{12}} \frac{1}{H(a(t)) - H(-a(t))}\,dt \\ &\geq 2.29461 \end{aligned}$$

where $H(s) = 2\arctan(\exp(s))$. □

From Proposition 8.5, Proposition 8.7 and Remark 8.4, we immediately derive the following result.

Corollary 8.8. *The extremal nonpositively curved Dyck's surface $\mathcal{D}_{\leq 0}$ is not conformally equivalent to the extremal hyperbolic Dyck's surface $\mathcal{D}_{-1}$.*

Remark 8.9. Simpler bounds on the capacities of the collars can be derived both for $\mathcal{A}_{-1}$ and $\mathcal{A}_{\leq 0}$ as follows. The collar $\mathcal{A}_{-1}$ can be isometrically embedded into the bi-infinite hyperbolic cylinder with C as a simple geodesic loop. In this cylinder, the collar $\mathcal{A}_{-1}$ is contained in the tubular neighborhood U of C of width the length of the side opposite to a in the trirectangle T, *cf.* Figure 8.2. We deduce that the capacity of the collar $\mathcal{A}_{-1}$ is bounded from below by the capacity of U for which a formula has been established by Buser and Sarnak [11, p. 37]. Even more directly, the capacity of the collar $\mathcal{A}_{\leq 0}$ is bounded from above by twice the area of $\mathcal{D}_{\leq 0}$. However, none of these estimates is strong enough for our purpose. This explains why we made use of finer estimates.

Acknowledgments

We are grateful to Bjoern Muetzel, Hugo Parlier and Robert Silhol for helpful comments.

References

[1] Bangert, V.; Katz, M.; Stable systolic inequalities and cohomology products. *Comm. Pure Appl. Math.* **56** (2003), 979–997. See arXiv:math.DG/0204181.

[2] ———, An optimal Loewner-type systolic inequality and harmonic one-forms of constant norm. *Comm. Anal. Geom.* **12** (2004), no. 3, 703-732. arXiv:math.DG/0304494

[3] Bavard, C.: Inégalité isosystolique pour la bouteille de Klein. *Math. Ann.* **274** (1986), no. 3, 439–441.

[4] Bavard, C.: Inégalités isosystoliques conformes, *Comment. Math. Helv.* **67** (1992), no. 1, 146–166.

[5] Blatter, C.: Über Extremallängen auf geschlossenen Flächen. *Comment. Math. Helv.* **35** (1961), 153–168.

[6] Blatter, C.: Zur Riemannschen Geometrie im Grossen auf dem Möbiusband. *Compositio Math.* **15** (1961), 88–107.

[7] Bolza, O.: On binary sextics with linear transformations into themselves. *Amer. J. Math.* **10** (1887) 47–70.

[8] Burago, D.; Ivanov, S.: Riemannian tori without conjugate points are flat. *Geom. Funct. Anal.* **4** (1994), no. 3, 259–269.

[9] ———, On asymptotic volume of tori. *Geom. Funct. Anal.* **5** (1995), no. 5, 800–808.

[10] Buser, P.: Geometry and spectra of compact Riemann surfaces. Reprint of the 1992 edition. Modern Birkhäuser Classics. Birkhäuser Boston, Inc., Boston, MA, 2010.

[11] Buser, P.; Sarnak, P.: On the period matrix of a Riemann surface of large genus. With an appendix by J. H. Conway and N. J. A. Sloane. Invent. Math. 117 (1994), no. 1, 27–56.

[12] Calabi, E.: Extremal isosystolic metrics for compact surfaces. Actes de la Table Ronde de Géométrie Différentielle, Sémin. Congr. 1 (1996), Soc. Math. France, 146–166.

[13] Farkas, H. M.; Kra, I.: Riemann surfaces. Second edition. *Graduate Texts in Mathematics* **71**. Springer-Verlag, New York, 1992.

[14] Gendulphe, M.: Paysage Systolique Des Surfaces Hyperboliques Compactes De Caracteristique -1. See arXiv:math/0508036

[15] Gromov, M.: Metric structures for Riemannian and non-Riemannian spaces. Based on the 1981 French original. With appendices by M. Katz, P. Pansu and S. Semmes. Translated from the French by Sean Michael Bates. Reprint of the 2001 English edition. Modern Birkhäuser Classics. Birkhäuser Boston, Inc., Boston, MA, 2007.

[16] Horowitz, C.; Katz, Karin Usadi; Katz, M.: Loewner's torus inequality with isosystolic defect. *Journal of Geometric Analysis* **19** (2009), no. 4, 796-808. See arXiv:0803.0690

[17] Jenni, F.: Über den ersten Eigenwert des Laplace-Operators auf ausgewählten Beispielen kompakter Riemannscher Flächen. *Comment. Math. Helv.* **59** (1984), no. 2, 193–203.

[18] Katz, M.: Systolic geometry and topology. With an appendix by Jake P. Solomon. *Mathematical Surveys and Monographs*, **137**. American Mathematical Society, Providence, RI, 2007.

[19] Katz, M.; Sabourau, S.: An optimal systolic inequality for $CAT(0)$ metrics in genus two. *Pacific J. Math.* **227** (2007), no. 1, 95-107.

[20] Katz, M.; Sabourau, S.: Hyperellipticity and systoles of Klein surfaces. *Geometriae Dedicata* **159** (2012), no. 1, 277–293.

[21] Klein, C.; Kokotov, A.; Korotkin, D. : Extremal properties of the determinant of the Laplacian in the Bergman metric on the moduli space of genus two Riemann surfaces. *Math. Z.* **261** (2009), no. 1, 73–108. See arXiv:math/0511217.

[22] Miranda, R.: Algebraic curves and Riemann surfaces. *Graduate Studies in Mathematics*, **5**. American Mathematical Society, Providence, RI, 1995.

[23] Muetzel, B.: Inequalities for the capacity of non-contractible annuli on cylinders of constant and variable negative curvature. *Geometriae Dedicata* (online first). See http://dx.doi.org/10.1007/s10711-012-9788-z
and arXiv:1105.5060v1

[24] Parlier, H.: Fixed-point free involutions on Riemann surfaces. *Israel J. Math.* **166** (2008), 297-311. See arXiv:math.DG/0504109

[25] Pu, P.M.: Some inequalities in certain nonorientable Riemannian manifolds, *Pacific J. Math.* **2** (1952), 55–71.

[26] Sakai, T.: A proof of the isosystolic inequality for the Klein bottle. *Proc. Amer. Math. Soc.* **104** (1988), no. 2, 589–590.

[27] Schmutz, P.: Riemann surfaces with shortest geodesic of maximal length. *Geom. Funct. Anal.* **3** (1993), no. 6, 564–631.

Department of Mathematics, Bar Ilan University, Ramat Gan 52900 Israel
E-mail address: katzmik@macs.biu.ac.il

Laboratoire d'Analyse et Mathématiques Appliquées, Université Paris-Est Créteil, 61 Avenue du Général de Gaulle, 94010 Créteil, France
E-mail address: stephane.sabourau@u-pec.fr